

Seasonal and Decadal Variability of Atmosphere Pressure in Arctic, its Statistical and Temporal Analysis

Konstantin Belyaev^{1,2}[0000-0003-2111-2709], Gury Mikhaylov²[0000-0002-4535-7180]
Alexey Salnikov^{3,2}[0000-0001-8669-9905] and Natalia Tuchkova²[0000-0001-6518-5817]

¹ Shirshov Institute of Oceanology of RAS, Nahimovskiy pr., 36, 117218, Moscow, Russia
² Dorodnicyn Computing Center FRC CSC of RAS, Vavilov str., 40, 11933, Moscow, Russia
³ Lomonosov Moscow State University, GSP-1, Leninskie Gory, 11999, Moscow, Russia
natalia_tuchkova@mail.ru

Abstract. The paper analyzes the statistical and temporal seasonal and decadal variability of the atmospheric pressure field in the Arctic region of Russia. Schemes for the frequency analysis of probability transitions for characteristics of stochastic-diffusion processes were used as the main research method. On the basis of the given series of 60 years long from 1948 to 2008, such parameters of diffusion processes as the mean (drift process) and variance (diffusion process) were calculated and their maps and time curves were constructed. The seasonal and long-term variability of calculated fields was studied as well as their dependencies on a discretization of the frequency intervals. These characteristics were analyzed and their geophysical interpretation was carried out. In particular, the known cycles of solar activity in 11 and 22 years were revealed. Numerical calculations were performed on the Lomonosov-2 supercomputer of the Lomonosov Moscow State University.

Keywords: Time Series Analysis, Random Diffusion Processes, Seasonal and Long-Term Variability of Atmospheric Pressure.

1 Introduction

Time series analysis (ATS) is one of the most well-developed and widely used areas in mathematical statistics. ATS methods are successfully applied in geophysics, economics, engineering and other types of human activity related to the study of data sets. For example, one of the first applications of ATS methods was the analysis of harvest data in England in the 18th century [1], associated with grain harvest, which was divided into a long-term trend, a seasonal component and an irregular component depending on current events (weather conditions, inflationary price splash, etc.). Subsequently, the ATS began to be used in the analysis of the financial market [2], in the analysis of long-term variability of geophysical characteristics, such as the temperature of air or water [3], in more complex models and schemes [4]. At the present stage of the ATS analysis for instance, autoregressive and moving average (ARIMA) schemes are often used [5].

Copyright © 2020 for this paper by its authors.

Use permitted under Creative Commons License Attribution 4.0 International (CC BY 4.0).

However, this one requires the use of a large amount of computing power, computer time and memory, solving problems of visualizing the results, and many related problems. In recent years, thanks to significant progress in the field of computing systems and numerical modeling, accumulation and processing of big data, experiments on ATS have become available to many research groups and individual users belonging to a certain scientific community. This, in turn, contributes to the further development of numerical modeling, analysis of modeled data and their obtained results with the further comparison.

Research on ATS is also widely used directly in probability theory and mathematical statistics. One of the methods of analysis is the representation of the series in the form of a Markov chain and / or a Markov process. Since the literature on Markov processes is very extensive, we will mention only a few of the most famous works in this area, which, however, set out all the necessary theoretical provisions and practical methods for calculating the characteristics necessary for further research. For example, [6] describes all the theoretical information needed in this work on how to determine the process parameters given below, and [7] provides specific examples of such processes.

In this work, the behavior of the atmospheric pressure field is modeled on the basis of the Markov diffusion process. Such processes describe well the behavior of the characteristics of fields that change under the influence of two forces - a short-period one, called process diffusion, and a long-period one, called drift. These models generalize the decomposition of a time series into a trend, periodic and random component, presented earlier in the literature, mentioned in [1], [3, 4]. In probability theory, such processes are described by stochastic differential equations [6, 7], and their probability densities are given by solutions of the Fokker–Planck–Kolmogorov equation [8].

The characteristics of those processes are adequately described by such models if two basic conditions are met. First, the increment (that is, the difference between two sequential points in time) should be much less than the total length of the row, and secondly, the field of these characteristics should be sufficiently uniform, that is, the behavior at neighboring points in space does not differ much from each other, especially if this behavior is viewed over long intervals. For the atmospheric pressure field in a relatively small region, which we are considering, these conditions are satisfied. The length of the row is 60 years, while the time step, that is, the increment, is one day. And the size of the cyclonic atmospheric formation, which basically forms the pressure field, is comparable to the dimensions of the entire area under consideration, that is, inside the area for one formation it does not change much. It is important to investigate to what extent the result depends on the division of the actually observed pressure interval (that is, the difference between the maximum and minimum pressure in the entire area) into separate sub-intervals, which are used to calculate the frequency (statistical) characteristics when analyzing the variability of this field.

Methods of diffusion stochastic processes were previously used for various problems, including for data assimilation problems, in the methods proposed by the authors [9, 10]. However, this method has not been widely used to describe the seasonal and long-term behavior of atmospheric processes.

The work did the following:

- the characteristics of the models are built, their features are described, in particular the features of the seasonal and long-term course, the analysis of the features is carried out;

- time graphs and spatial maps of these characteristics were built, and their analysis was carried out.

- the analysis of resistance to the division of the entire pressure interval (maximum minus minimum of the field over the entire region) into frequency sub-intervals was carried out.

2 Probability model

The variability of a random process, (in our case this is a pressure field), is represented in the form

$$dX = a(t, X)dt + b(t, X)dW, \quad (1)$$

where X is a pressure value at moment t and at point with given coordinates, this is not explicitly shown, t is a time, dW is a standard notation of Gaussian ‘white noise’, that is the generalized random process with zero average and variance equaled 1. Its covariance function is equaled to delta-function, that is the following $EdW(t)dW(\tau) = \delta(t - \tau)$. Hereafter, $\delta(t - \tau) = 1$, if $t = \tau$ or zero otherwise. Besides that, $a(t, x)$, $b(t, x)$ are some functions which are calculated according to the work [6]. An expression (1) is understood as

$$X(t + \Delta t) - X(t) = \int_t^{t+\Delta t} a(u, X)du + \int_t^{t+\Delta t} b(u, X)[W(u + du) - W(u)]. \quad (2)$$

In (2) the expression represents the Gaussian random variable $W(u + du) - W(u)$ with zero average and variance du . The stochastic integral theory and all definitions needed to understand formulae (1) and (2) can be found in [6, 7].

According to [6], for definition of coefficients $a(t, x)$ and $b(t, x)$ the following formulae are used

$$a(t, x) = (dt)^{-1} \int_t^{t+dt} (y - x)p(y | x)dy, \quad (3)$$

$$b^2(t, x) = (dt)^{-1} \int_t^{t+dt} (y - x)^2 p(y | x)dy, \quad (4)$$

where, x and y are the values of the process $X(t)$ at moment t and $t + dt$, respectively; $p(y | x)dt$ is the probability (conditional probability) of an event that the values

$X(t + dt) = y$ with condition $X(t) = x$, that is $p(y|x)dt = P(X(t + dt) = y | P(t) = x)$. The problem is posed: to calculate these probabilities and to perform their analysis.

To statistically determine the conditional probability, one need to have a sample of observations (values) x and y at a fixed point in space. However, since the area under consideration is homogeneous, as noted above, points with these values can be marked throughout this area. Namely, the technique for determining these probabilities is as follows: at step t , all points in the region are marked where $X(t) = x$ ($x_{\min} < x < x_{\max}$). For simplicity, the values x_{\min} , x_{\max} can be considered the same for all t . Let there be $n(x)$ such points. Further, at step $t + dt$ at those and only at those points where $X(t) = x$ all points are selected where $X(t + dt) = y$. Let there be $m(y)$ such points. Then $p(y|x)dt = m(y)/n(x)$. Obviously it really is a probability. Further, the calculation of the coefficients is carried out according to formulas (3) and (4). Such a method for determining the coefficients was previously published for a slightly different problem in [9, 10]. In this case, as can be seen from the description of the method, the result depends on the number of sub-intervals into which the entire interval of the pressure field variability is divided (that is, the maximum minus the minimum of the field over the area). Experiments were carried out on splitting into 20 and 60 intervals. Also, to avoid the unrealistic case $n(x) = 0$, the sub-intervals were selected such as to choose at least one value of $X(t)$ in each sub-interval.

3 Observational data and computation results

The paper considers the field of atmospheric pressure in the area bounded by coordinates 62°N-80°N and 30°E-90°E, that is, the region of Russia, from the Baltic coast near St. Petersburg to Severnaya Zemlya and the Yenisei in Siberia. On the one hand, this region is wide enough to neglect the local features of atmospheric processes; on the other hand, it is sufficiently homogeneous, since the sizes of large atmospheric formations are comparable to the dimensions of the entire region. By time, pressure data were recorded from January 1, 1948 to December 31, 2008, daily in a one-degree grid. The data were obtained at the Hydrometeorological Center of Russia (HMC) and were used earlier in some works, for example, in [11].

Fig. 1(a-d) presents the pressure fields in the considered area on January 1, with the time-interval 20 years (1948–2007).

Figures 1 demonstrate that the pressure fields have the long-term variability but homogeneous enough with respect to the space, since the areas of approximately equaled pressure take most of space domain. Some exemption can be seen in 1987 but even in this case the pressure gradient is not large, its value is approximately 10 gpa per 1000 km. Therefore, this field may be considered as homogeneous with the large confidence level and the aforementioned methods can be applied.

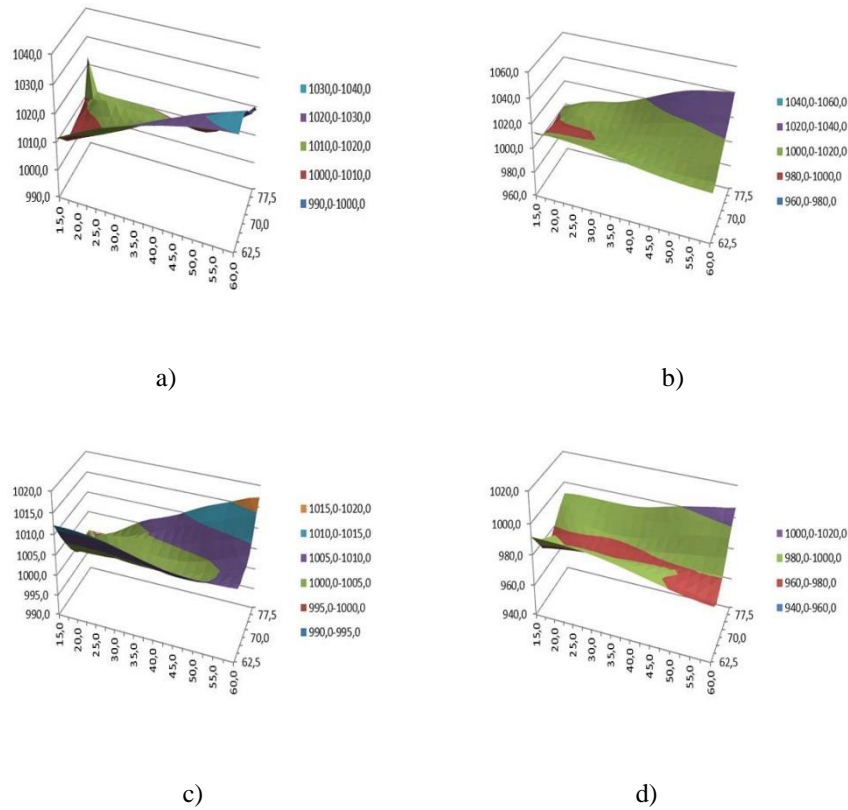


Fig. 1. Observed pressure fields in the considered area on January 1: a) 1948, b) 1967, c) 1987, d) 2007 years.

According to the given observational data, using formulas (3) and (4), the coefficients were constructed for each X as the pressure values in the considered area for a specific day. In this case, the division of the entire range of pressure values was carried out into 20 and 60 intervals. We present only the 60 sub-interval discretization.

The next figures illustrate the behavior of average value of coefficients $a(t, x)$ and $b(t, x)$, their seasonal and decadal variability.

Fig. 2(a-d) shows the behavior of the average coefficient $a(t, x)$ for 2007 when divided into 20 intervals. From formula (1) it is seen that the average for the process dX will be $a(t, x) = 0$. However, the sample mean $a(t, x)$ may not coincide with the theoretical mean, and this difference needs to be analyzed. 2007 is taken as indicative, in other years the picture is similar. In these figures, it is noteworthy that the spread of the coefficient $a(t, x)$ around the mean value equal to zero is very small in summer, in July, and rather large in the transitional months – April and October, especially in October. Moreover, the deviation from zero is generally positive. This means that atmospheric formations (cyclones and anticyclones) in the area under consideration mainly change

in the direction of increasing pressure, that is, the incoming cyclone (and most of them) does not deepen, that is, the pressure does not decrease.

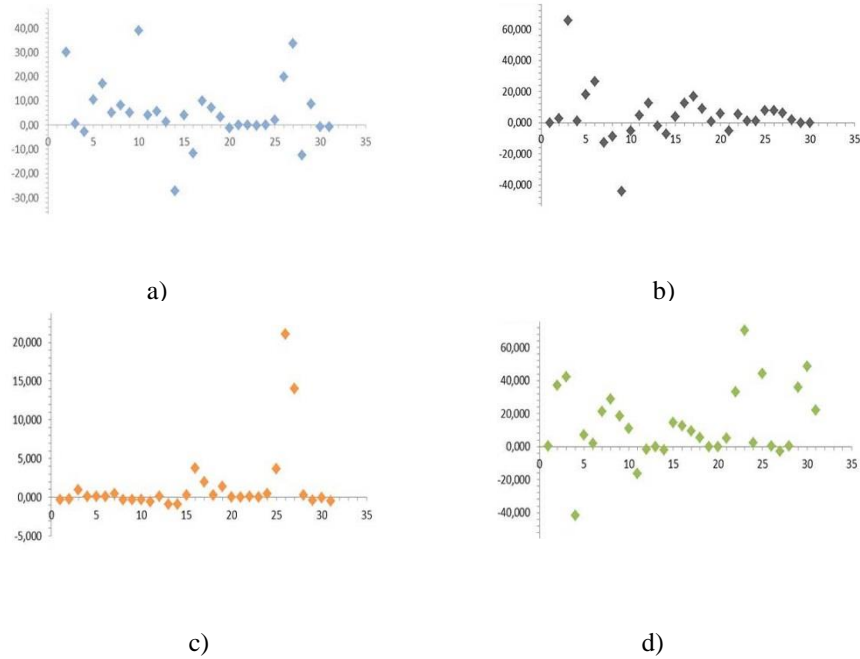


Fig. 2. Behavior of the average coefficient $a(t, x)$, for 2007 year a) January; b) April; c) July; d) October.

Fig. 3 shows the annual variability for the $a(t, x)$ on January 15 during the period 1948–2008 years. The long-term variability of the pressure increment expressed in values of $a(t, x)$, taken on 15 of each months demonstrates that there are the quasi-periodical oscillations with well-pronounced 11-year cycle and a weakly pronounced quasi-biannual cycle. These cycles are very well-known in geoscience and caused both solar activity and biannual wind and baric oscillations, cited by many authors, for instance [12].

One may note that in the beginning of calculations, in 1948 year the graphs contains the sharp splash which will not observe further. This can be explained due to the existence of noise and badly processed data in the beginning of the archive. Then all data are extensively processed, cleaned and smoothed.

Fig. 4 (a-d) shows the behavior of the average coefficient $b^2(t, x)$ for 2007 year and Fig. 5 contains the annual variability for this coefficient calculated at January 15 during entire period.

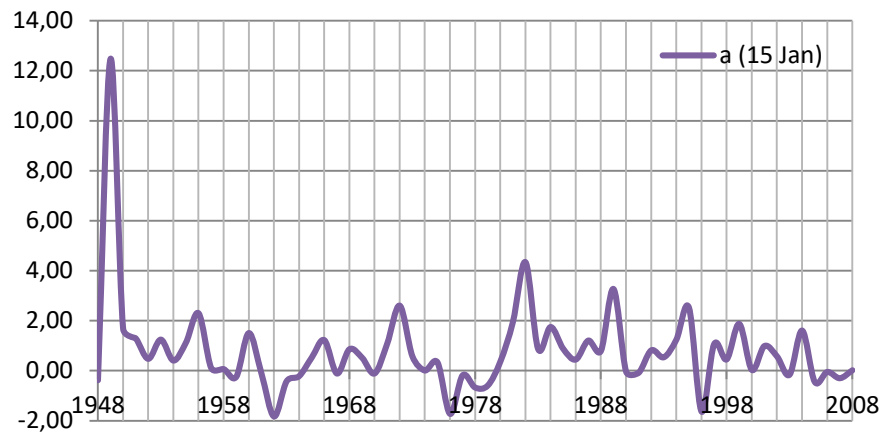


Fig. 3. Graph for coefficient $a(t, x)$ from 1948 until 2008 years (measured at 0 o'clock Jan 15).

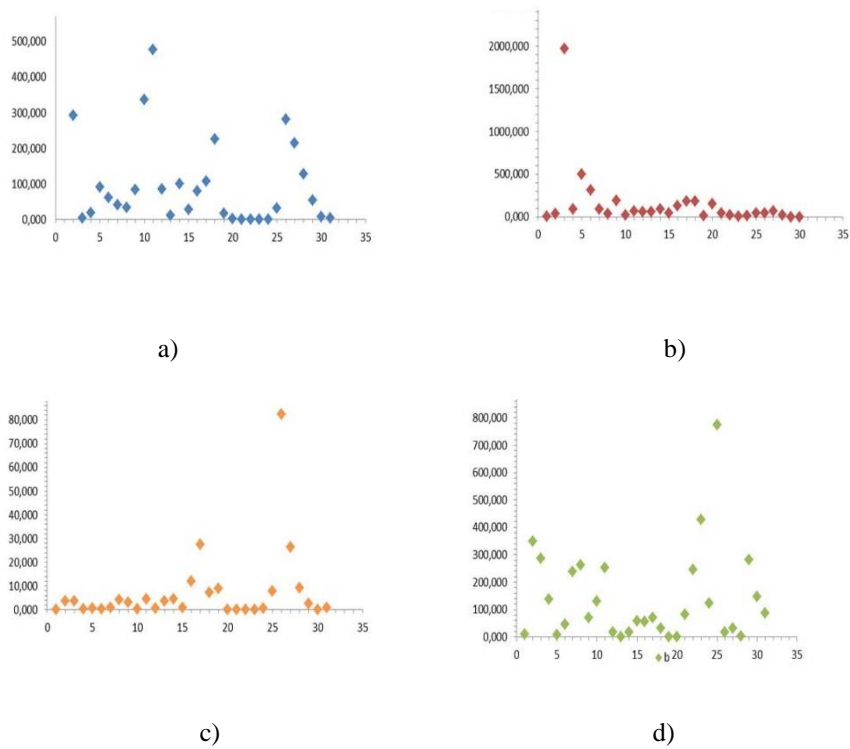


Fig. 4. Behavior of $b^2(t, x)$, for 2007 year: a) January; b) April; c) July; d) October.

Figs. 3 and 4 demonstrate the tendencies in ice fraction for 2 different time-periods. Fig. 3 shows the model prediction on 2027 started from 2000 and Fig. 4 shows the difference between 1965–2016 for low resolution model. It is clearly visible the tendency to the ice thickness everywhere in Arctic except some zones in the East of Russia and to the eastward from Novaya Zemlya. The low resolution model shows the global fall of ice thickness during 40-year period everywhere except Severnaya Zemlya archipelago. Some questions arise the slight increase of the ice thickness in Baltic Sea but this can be explained because the increase is not significant, it is about 30 cm and this is really observed in January.

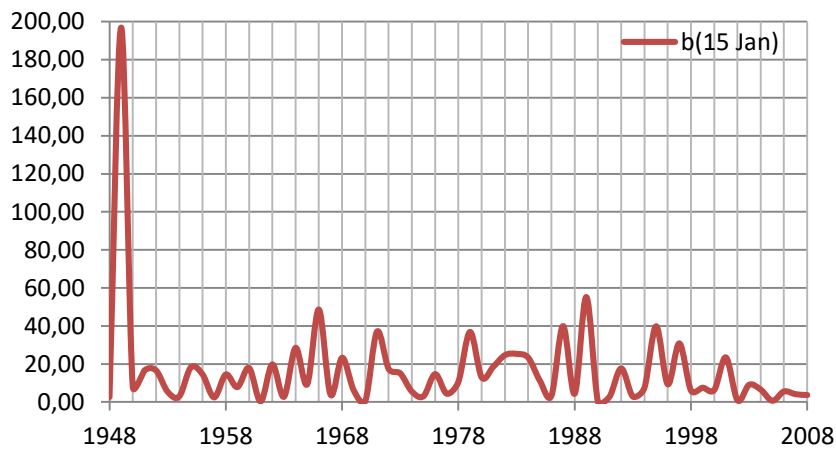
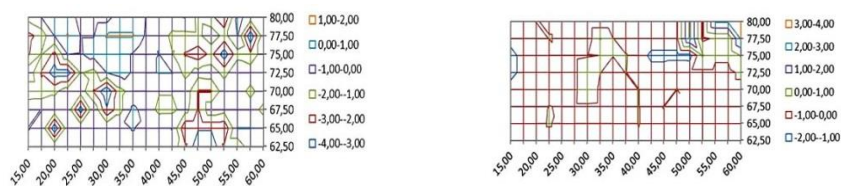


Fig. 5. Graph for coefficient $b^2(t, x)$ from 1948 until 2008 years (measured at 0 o'clock Jan 15).

In Figs. 4 and 5 one can see that the coefficient $b^2(t, x)$ quite well corresponds to the coefficient $a(t, x)$, with some differences. So, from Fig. 5 that the seasonal variation for the coefficient $b^2(t, x)$ is less pronounced, for example, it is almost invisible in April or July, and the interannual variation reflects the 11-year cycle worse (although it also exists) and the quasi-biannual cycle is better than the coefficient $a(t, x)$. Neither coefficient $a(t, x)$ nor $b^2(t, x)$ contain any linear trends. There is also a strong surge in 1948, explained above.

Fig. 6 shows the spatial location of the coefficient $a(t, x)$, a total of 4 values for January 15, 1948, 1968, 1988 and 2008, interval 20 years.

It is seen that the jumps in the values of this coefficient are sufficiently localized and do not exceed 5 gpa/day with different signs. The spatial arrangement of this coefficient over the area is uniform, no noticeable localization zones are observed, and it should also be noted that the isolines of the values of the coefficient $a(t, x)$ are quite local in comparison with the dimensions of the area itself (shown in different colors). This indicates the local cause of pressure changes on a large scale.



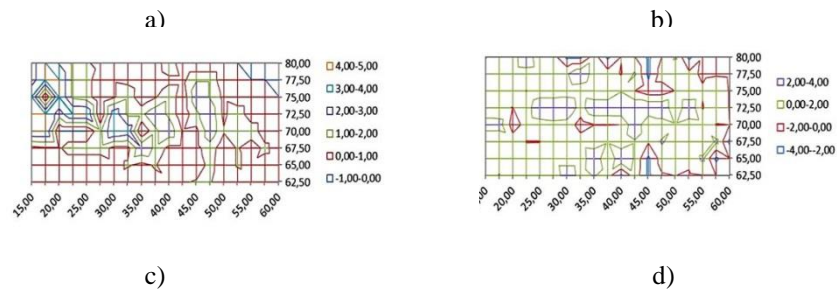


Fig. 6. Coefficient $a(t, x)$ on January 15: a) 1948; b) 1968; c) 1988; d) 2008 years.

The coefficient $b^2(t, x)$ (Fig. 7) is more chaotic, its distribution over space is not as common as for the coefficient $a(t, x)$. In addition, it can be concluded that the spatial location of the coefficient $b^2(t, x)$ is more localized and concentrated in continuous zones (except for the values for 2008). In terms of amplitude, the range of this coefficient is significantly larger than for the coefficient $a(t, x)$, but locally it occupies a smaller size of the entire area.

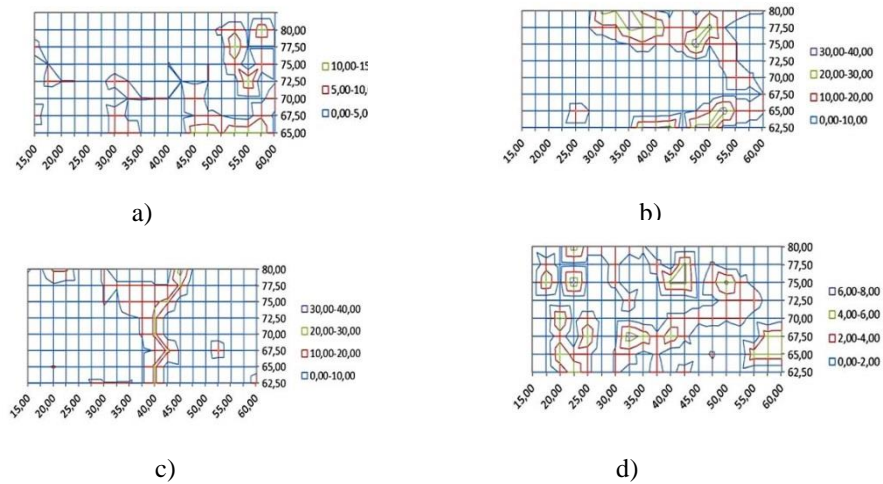


Fig. 7. Coefficient $b^2(t, x)$ for January 15: a) 1948; b) 1968; c) 1988; d) 2008 years.

It can also be noted that with an increase in the discretization into the number of intervals, graphs 3 and 5 become smoother, Figs. 4 and 6 are more pronounced, but they qualitatively coincide. Therefore, the results of the work are qualitatively independent of the number of divisions. However, for the correctness and reliability of the calculations, it is required that, when the whole interval is broken down, each sub-interval must contain at least one observation, so that the conditional probabilities can be correctly calculated using formulas (3) and (4).

4 Conclusions and Outlook

Several characteristics were obtained in this study that reflect both long-term and short-term behavior of the pressure increment in the Northern region of Russia over 60 years. Knowledge of such characteristics is very useful for medium and long-term forecasts of weather and climate change, as well as for modeling the dynamics of currents in the North Seas of Russia, especially when calculating pilotage along the Northern Sea Route. In addition, the knowledge and forecast of the characteristics obtained in the work will make it possible to calculate and determine the confidence limits of possible pressure values, and hence a number of derivatives of this value, for example, geostrophic wind, which will allow applying this knowledge in determining extreme values, such as strong winds, extreme waves and a number of other characteristics.

This work was carried out with partial support from the Russian Foundation for Basic Research, project 18-29-10085 mk and within the framework of the topics 0149-2019-0004, and ‘Mathematical methods for data analysis and forecasting’.

References

1. Kendall, M., Stuart, A., Ord, J.K.: The Advanced Theory of Statistics. Volume 3: Design and Analysis, and Time-Series. Fourth edition (1983).
2. Murphy, J.: Technical analysis of the futures markets. A Comprehensive Guide to Trading Methods and Applications. New York Institute of Finance (1986).
3. Prival'skij, V.E.: Statisticheskaya predskazuemost' srednej godovoj temperatury vozduha severnogo polushariya. Doklady AN SSSR, 257 (6), 1342–1345 (1981).
4. Belyaev, K.P., Muzychenko, A.C., Selemenov, K.M.: Statisticheskie harakteristiki formirovaniya anomalij poverhnostnoj temperatury vody. Sb. Statisticheskie zakonomernosti klimaticheskoj izmenchivosti okeanov, red. Lappo S.S. Gidrometizdat, Leningrad, 65-72 (1988).
5. Balasmeh, O., Babbar, R., Karmaker, T.: Trend analysis and ARIMA modeling for forecasting precipitation pattern in Wadi Shueib catchment area in Jordan. Arabian Journal of Geosciences, 12, 27 (2019). <https://doi.org/10.1007/s12517-018-4205-z>.
6. Gihman, I., Skorohod, A.: Vvedenie v teoriyu sluchajnyh processov. Nauka, Moscow (1965).
7. Nazarov, A., Terpunov, A.: Teoriya veroyatnostej i sluchajnyh processov. Izd-vo Tomskogo Gosuniversiteta (2010).
8. Risken, H.: The Fokker–Planck Equation: Methods of Solutions and Applications. Springer (1984).

9. Belyaev, K., Kuleshov, A., Tanajura, K., Tuchkova, N.: Metod korrekcii raschetov dinamicheskoy modeli dannymi nablyudenij i ego primenenie k analizu dinamiki Atlanticheskogo okeana. *Matematicheskoe Modelirovanie*, 27 (2), 20–32 (2015).
10. Tanajura, C.A.S., Belyaev, K.: On the oceanic impact of a data-assimilation method in a coupled ocean-land-atmosphere model. *Ocean Dynamics*, 52 (3), 123–132 (2002).
11. Popov, S.K.: Vliyanie morskogo l'da na prilivnye kolebaniya urovnya morya i skorosti techenij v Barencevom i Belom moryah. *Trudy Gidrometcentra RF, Gidrometeorologicheskie issledovaniya i prognozy*, 4 (370), 137–155 (2018).
12. Devyatova, E.V., Mordvinov, V.I.: Kvazidvuhletnee kolebanie vetra v nizkoshirotnoj stratosfere i volnovaya aktivnost' atmosfery zimoj v severnom polusharii. *Izvestiya RAN FAO*, 47(5), 608–621 (2011).